

Numerical validation and properties of a rapid binding approximation of a target-mediated drug disposition pharmacokinetic model

Anshu Marathe · Wojciech Krzyzanski · Donald E. Mager

Received: 5 March 2009 / Accepted: 16 April 2009 / Published online: 12 May 2009
© Springer Science+Business Media, LLC 2009

Abstract Target mediated drug disposition (TMDD) describes the phenomenon where high affinity binding of a drug to its pharmacological target (enzymes or receptors) significantly alters the pharmacokinetic profile of the drug. A rapid binding model replaces the often inestimable binding micro-constants (k_{on} and k_{off}) of TMDD models with the equilibrium dissociation constant (K_D) by assuming rapid binding of the drug to its target. The purpose of this study is to examine the validity of the rapid binding assumption and the pharmacokinetic properties of this model. Temporal profiles of free drug in plasma and a non-specific distribution site, free receptor, and the pharmacodynamically relevant, drug–receptor complex obtained from the rapid binding model compared favorably with the full TMDD model for small values of the parameter ε , which represents the ratio of the time required for drug–receptor binding relative to the time required for drug to be cleared from the system. The effect of escalating drug doses on the temporal characteristics and the comparison between the two models has been numerically investigated. A closer match between the full and rapid binding models is observed for high doses. Analysis for very large doses (Dose/V_c) relative to endogenous steady-state receptor concentration (R_{ss}), reveals that the rapid binding model reduces to a standard two compartmental model with a plasma compartment with linear drug elimination and a peripheral compartment. Decreasing clearance with increasing dose and decreasing R_{ss} indicates that for drugs exhibiting TMDD, the relative ratio of R_{ss} and dose is an important determinant of the pharmacokinetic properties rather than the individual parameters alone. An analytical solution derived for clearance shows that the primary elements of the apparent clearance of the drug are the linear

Electronic supplementary material The online version of this article (doi:[10.1007/s10928-009-9118-8](https://doi.org/10.1007/s10928-009-9118-8)) contains supplementary material, which is available to authorized users.

A. Marathe · W. Krzyzanski · D. E. Mager (✉)
Department of Pharmaceutical Sciences, University at Buffalo, State University of New York, 543
Hochstetter Hall, Buffalo, NY 14260, USA
e-mail: dmager@buffalo.edu

clearance given by $k_{el}V_c$, the non-linear clearance due to drug–receptor complex internalization (k_{int}), and the ratio of AUC values of the receptor complex to that of free drug. Overall, simulations and analytical techniques applied here provide a better understanding of the validity of the rapid binding model and provide guidelines for its application.

Keywords Nonlinear pharmacokinetics · Drug-receptor binding · Target mediated drug disposition

Introduction

Target mediated drug disposition (TMDD) is a phenomenon where binding of a drug with high affinity to its pharmacological target (receptor or enzyme) significantly influences the apparent pharmacokinetic properties of the drug, typically resulting in a decrease in the steady state volume of distribution (V_{ss}) with increasing dose levels [1]. A decrease in clearance (CL) may also be observed when the binding process initiates a major drug elimination pathway [2], such as receptor mediated endocytosis, which is important for many polypeptides and hormones [3]. These pharmacokinetic parameters approach a limiting value with dose, owing to a saturable capacity limitation of the pharmacological target. Target-mediated disposition is now recognized as a major determinant of the distribution and elimination of various proteins, peptides, and monoclonal antibodies that interact with specific high-affinity biological targets [4, 5].

A general pharmacokinetic model of TMDD was proposed to better understand the behavior of such systems [2]. This model has been applied to characterize the disposition of several drugs, ranging from small to macro-molecules, and has been reviewed elsewhere [6]. The approach has been extended to nonlinear mixed effects modeling as well to analyze and interpret population PK/PD data [7, 8]. One major limitation of the model is that the drug binding micro-constants (k_{on} and k_{off}) that are included in the model may not be easily estimated from routine pharmacokinetic data. Thus, a model was introduced which replaces these micro-constants by an equilibrium dissociation constant (K_D) by assuming rapid binding of the drug to its target [9]. The rapid binding model was successfully tested against previously published data of leukemia inhibitory factor (LIF) in sheep which was earlier characterized by the TMDD model [10].

Mathematical approximations to complex models are common in the analysis of biological and pharmacological systems, particularly when the numerical identifiability of specific parameters becomes untenable. The classical Michaelis–Menten approximation is extensively used in biochemistry and pharmacology to understand the non-linear kinetics of enzymatic reactions and specific and non-specific protein binding. Various forms of the Michaelis–Menten equation have also been successfully used to characterize aspects of some TMDD systems [11–13]; however, some pharmacological processes, such as drug-target turnover, may necessitate a TMDD model [14]. Other study design and assay characteristics can also influence the selection between Michaelis–Menten and TMDD systems, such as the range of dose

levels and the lower limit of quantification [15]. Whereas significant work has been done to understand the limitations and domain of validity of the quasi-steady state approximation in enzyme kinetics [16–18], to our knowledge, similar techniques have yet to be applied to the rapid-binding approximation to TMDD models.

The purpose of this study is to numerically test the validity of the rapid binding assumption. Computer simulations were performed to compare the temporal profiles of the free drug concentration in plasma, the drug in a peripheral tissue compartment, the free receptor concentration, and the drug–receptor complex from the rapid binding model and the TMDD model for a range of parameter values (ϵ) representing different time scales for drug–receptor binding. The effect of several kinetic parameters and dose on the accuracy of the approximation is also examined. The simultaneous effect of the dose and the endogenous receptor concentration on drug clearance was evaluated. The limits for clearance and steady-state volume of distribution of the drug at large doses relative to receptor concentration were analytically derived. Thus, simulations and analytical mathematical techniques in this study provide a better understanding of the validity and the pharmacokinetic properties of the rapid binding model.

Theoretical

A general pharmacokinetic model of TMDD was proposed and is illustrated in Fig. 1 [2]. The model assumes that drug on reaching the central compartment (C) binds at a second order rate (k_{on}) to free receptor (R) to form the drug–receptor complex (RC), which in turn, dissociates by a first-order rate process (k_{off}). The internalization and degradation of the drug–receptor complex, which can reflect receptor mediated endocytosis [3], is included as a first-order rate process (k_{int}). Drug in the central compartment undergoes linear distribution to a non-specific tissue compartment (A_T) by first-order processes (k_{pt} , k_{tp}) as well as first-order elimination (k_{el}). Receptor turnover is modeled by zero-order production (k_{syn}) and first-order degradation (k_{deg}). Whereas various functions are available for routes of drug administration, this paper considers only bolus intravenous (IV) injection. The model equations are as follows [2]:

$$\frac{dC}{dt} = -(k_{el} + k_{pt})C + k_{tp} \frac{A_T}{V_c} - k_{on}R \cdot C + k_{off}RC \tag{1}$$

$$\frac{dA_T}{dt} = k_{pt}CV_c - k_{tp}A_T \tag{2}$$

$$\frac{dR}{dt} = k_{syn} - k_{on}R \cdot C - k_{deg}R + k_{off}RC \tag{3}$$

$$\frac{dRC}{dt} = k_{on}R \cdot C - (k_{off} + k_{int})RC \tag{4}$$

where V_c denotes the volume of the central compartment. It is assumed that no free drug is present endogenously prior to the IV bolus, therefore the initial conditions for Eqs. 1–4 are defined as:

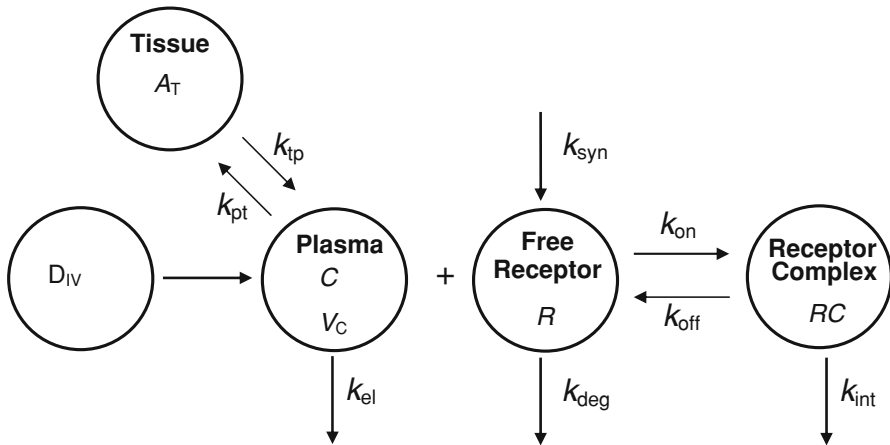


Fig. 1 Pharmacokinetic model of target mediated drug disposition. Drug administered as an IV bolus (D_{IV}) into the central (plasma) compartment (C , V_C) reversibly distributes (k_{pt} , k_{tp}) to a non-specific tissue compartment (A_T), reversibly binds to a pharmacological target (R) to form a drug–receptor complex (RC) and gets eliminated from the plasma (k_{el}). The model includes the synthesis (k_{syn}) and degradation (k_{deg}) of the pharmacological target and the internalization (k_{int}) of the drug–receptor complex

$$C(0) = \text{Dose}/V_C \quad (5a)$$

$$A_T(0) = 0 \quad (5b)$$

$$R(0) = R_{ss} \quad (5c)$$

$$RC(0) = 0 \quad (5d)$$

where R_{ss} is the steady-state endogenous free receptor concentration (i.e., k_{syn}/k_{deg}).

A major challenge in implementing the TMDD model is the estimation of the second-order association rate constant, k_{on} and the first-order dissociation rate constant, k_{off} . Thus, a rapid binding model was derived which replaces these microconstants with the equilibrium dissociation constant, K_D [9]. The rapid binding assumption provides a correlation between the free drug concentration in the plasma (C_{rb}), the free receptor concentration (R_{rb}), the drug–receptor complex concentration (RC_{rb}), and K_D as given by:

$$\frac{R_{rb} \cdot C_{rb}}{RC_{rb}} = K_D \quad (6)$$

The subscript rb represents rapid binding. The system is parameterized based on total drug and receptor concentrations ($C_{tot,rb}$ and $R_{tot,rb}$), which are defined as:

$$C_{tot,rb} = C_{rb} + RC_{rb} \quad (7)$$

$$R_{tot,rb} = R_{rb} + RC_{rb} \quad (8)$$

Thus, the set of differential equations describing the rapid binding model are as follows:

$$\frac{dC_{\text{tot,rb}}}{dt} = -k_{\text{int}}C_{\text{tot,rb}} - (k_{\text{el}} + k_{\text{pt}} - k_{\text{int}})C_{\text{rb}} + k_{\text{ip}}\frac{A_{\text{T,rb}}}{V_c} \tag{9}$$

$$\frac{dA_{\text{T,rb}}}{dt} = k_{\text{pt}}C_{\text{rb}}V_c - k_{\text{ip}}A_{\text{T,rb}} \tag{10}$$

$$\frac{dR_{\text{tot,rb}}}{dt} = k_{\text{syn}} - (k_{\text{int}} - k_{\text{deg}})(C_{\text{tot,rb}} - C_{\text{rb}}) - k_{\text{deg}}R_{\text{tot,rb}} \tag{11}$$

$$C_{\text{rb}} = \frac{1}{2} \left[(C_{\text{tot,rb}} - R_{\text{tot,rb}} - K_D) + \sqrt{(C_{\text{tot,rb}} - R_{\text{tot,rb}} - K_D)^2 + 4K_D C_{\text{tot,rb}}} \right] \tag{12}$$

where the free drug concentration C_{rb} (Eq. 12) is the solution to a quadratic equation obtained by substituting $C_{\text{tot,rb}}$ and $R_{\text{tot,rb}}$ in Eq. 6:

$$\frac{[R_{\text{tot,rb}} - (C_{\text{tot,rb}} - C_{\text{rb}})] \cdot C_{\text{rb}}}{C_{\text{tot,rb}} - C_{\text{rb}}} = K_D \tag{13}$$

The initial conditions for Eqs. 9–11 are similar to Eq. 5:

$$C_{\text{tot,rb}}(0) = \text{Dose}/V_c \tag{14a}$$

$$A_{\text{T,rb}}(0) = 0 \tag{14b}$$

$$R_{\text{tot,rb}}(0) = R_{\text{ss}} \tag{14c}$$

Scaling

In order to perform a detailed numerical validation of the rapid binding model, the governing equations of the full TMDD model and the rapid binding model were scaled. Such scaling facilitates the comparison of temporal profiles of key variables from the two models. It also enables the linear independency of the parameters. The dimensionless variables for the TMDD model are defined as:

$$\tau = \frac{t}{t_{\text{char}}} \tag{15a}$$

$$c(\tau) = \frac{C(t)}{C_{\text{char}}} \tag{15b}$$

$$a_{\text{T}}(\tau) = \frac{A_{\text{T}}(t)}{C_{\text{char}}V_c} \tag{15c}$$

$$r(\tau) = \frac{R(t)}{R_{\text{char}}} \tag{15d}$$

$$rc(\tau) = \frac{RC(t)}{R_{\text{char}}} \tag{15e}$$

where t_{char} , C_{char} and R_{char} represent the scaling variables. The dimensionless variables for the rapid binding model are similarly defined as:

$$\tau = \frac{t}{t_{\text{char}}}; \quad (16a)$$

$$c_{\text{tot,rb}}(\tau) = \frac{C_{\text{tot,rb}}(t)}{C_{\text{char}}} \quad (16b)$$

$$a_{\text{T,rb}}(\tau) = \frac{A_{\text{T,rb}}(t)}{C_{\text{char}} V_c} \quad (16c)$$

$$r_{\text{tot,rb}}(\tau) = \frac{R_{\text{tot,rb}}(t)}{R_{\text{char}}} \quad (16d)$$

$$rc_{\text{rb}}(\tau) = \frac{RC_{\text{rb}}(t)}{R_{\text{char}}} \quad (16e)$$

$$c_{\text{rb}}(\tau) = \frac{C_{\text{rb}}(t)}{C_{\text{char}}} \quad (16f)$$

Appropriate choices for C_{char} and R_{char} would be Dose/V_c and R_{ss} as they represent the maximum possible ligand and free receptor concentration in the system. $1/k_{\text{el}}$ was considered as an appropriate choice for t_{char} as it directly correlates with linear clearance.

Scaled TMDD model equations

The governing equations of the TMDD model (Eqs. 1–4) in terms of the dimensionless variables (Eq. 15) and parameters are:

$$\frac{dc}{d\tau} = -(1 + \beta)c + \gamma a_{\text{T}} - \frac{\delta r \cdot c}{\varepsilon} + \frac{\delta \lambda rc}{\varepsilon} \quad (17)$$

$$\frac{da_{\text{T}}}{d\tau} = \beta c - \gamma a_{\text{T}} \quad (18)$$

$$\frac{dr}{d\tau} = \kappa - \frac{r \cdot c}{\varepsilon} - \kappa r + \frac{\lambda rc}{\varepsilon} \quad (19)$$

$$\frac{drc}{d\tau} = \frac{r \cdot c}{\varepsilon} - \frac{\lambda rc}{\varepsilon} - \mu rc \quad (20)$$

where

$$\beta = k_{\text{pt}}/k_{\text{el}} \quad (21a)$$

$$\gamma = k_{\text{tp}}/k_{\text{el}} \quad (21b)$$

$$\delta = \frac{k_{\text{syn}}}{k_{\text{deg}}(\text{Dose}/V_c)} \quad (21c)$$

$$\kappa = k_{\text{deg}}/k_{\text{el}} \quad (21d)$$

$$\lambda = \frac{K_{\text{D}}}{(\text{Dose}/V_c)} \quad (21e)$$

$$\mu = k_{int}/k_{el} \tag{21f}$$

$$\varepsilon = \frac{k_{el}}{k_{on}(Dose/V_c)} \tag{21g}$$

The dimensionless initial conditions for the above differential equations from Eq. 5 are:

$$c(0) = 1 \tag{22a}$$

$$a_t(0) = 0 \tag{22b}$$

$$r(0) = 1 \tag{22c}$$

$$rc(0) = 0 \tag{22d}$$

Scaled rapid binding model equations

The governing equations of the rapid binding model (Eqs. 6–12) in terms of the dimensionless variables (Eq. 16) and parameters (Eq. 21) are:

$$\frac{r_{rb} \cdot c_{rb}}{rc_{rb}} = \lambda \tag{23}$$

$$\frac{dc_{tot,rb}}{d\tau} = -\mu c_{tot,rb} - (1 + \beta - \mu)c_{rb} + \gamma a_{T,rb} \tag{24}$$

$$\frac{da_{T,rb}}{d\tau} = \beta c_{rb} - \gamma a_{T,rb} \tag{25}$$

$$\frac{dr_{tot,rb}}{d\tau} = \kappa - \frac{(\mu - \kappa)}{\delta} (c_{tot,rb} - c_{rb}) - \kappa r_{tot,rb} \tag{26}$$

$$c_{rb} = \frac{1}{2} \left[(c_{tot,rb} - \delta r_{tot,rb} - \lambda) + \sqrt{(c_{tot,rb} - \delta r_{tot,rb} - \lambda)^2 + 4\lambda c_{tot,rb}} \right] \tag{27}$$

where $c_{tot,rb}$ and $r_{tot,rb}$ are represented as:

$$c_{tot,rb} = c_{rb} + \delta rc_{rb} \tag{28}$$

$$r_{tot,rb} = r_{rb} + rc_{rb} \tag{29}$$

The dimensionless initial conditions for the above differential equations are:

$$c_{tot,rb}(0) = 1 \tag{30a}$$

$$a_{T,rb}(0) = 0 \tag{30b}$$

$$r_{tot,rb}(0) = 1 \tag{30c}$$

Rapid binding assumptions

Based on these characteristic scales, $k_{on}(Dose/V_c)$ represent the first-order rate of receptor pool depletion and its reciprocal, $\tau_B = 1/(k_{on}(Dose/V_c))$ represents the mean residence time of the receptor in the receptor compartment before binding to the drug. For many ligands, receptor binding tends to occur in time scales on the order

of seconds, whereas, much longer times are required for drug elimination. Mathematically, the binding is fast if $\tau_B \ll 1/k_{el}$ or the ratio, $\tau_B/(1/k_{el}) = k_{el}\tau_B = \varepsilon \ll 1$ is small. The accuracy of the model is also dependent on the assumption that the steady-state endogenous level of free receptor (R_{SS}) is comparable to $Dose/V_C$. Mathematically, this is represented as $R_{SS} = O(Dose/V_C)$ or $\delta = O(1)$ [9].

Methods

Simulations were performed to compare the temporal profiles of key variables from the TMDD and the rapid binding model using MATLAB (The Mathworks Inc., Natick, MA). Differential equations were solved numerically using ODE solver ode15s. The effect of increasing values of parameters (ε , β , γ , δ , κ , λ , and μ) on the match between the dimensionless concentration-time profiles of the free drug (c , c_{rb}), free receptor (r , r_{rb}), the drug receptor complex (rc , rc_{rb}) and drug in the tissue compartment (a_T , $a_{T,rb}$) from both models was assessed. The state variables, c , r , rc and a_T were obtained by numerically solving Eqs. 17–22. c_{rb} is calculated using Eq. 27, where the variables $c_{tot,rb}$, $a_{T,rb}$ and $r_{tot,rb}$ are obtained by numerically solving Eqs. 24–26. $rc_{rb} (= \{c_{tot,rb} - c_{rb}\}/\delta)$ and $r_{rb} = (r_{tot,rb} - rc_{rb})$ are obtained by rearranging Eqs. 28–29. Similarly, the effect of increasing IV doses of leukemia inhibitory factor (LIF) on the temporal profiles of free drug (C , C_{rb}), free receptor (R , R_{rb}), the drug receptor complex (RC , RC_{rb}) and drug in the tissue compartment (A_T , $A_{T,rb}$) was compared between the two models. State variables C , R , RC and A_T were obtained by numerically solving the dimensional Eqs. 1–4. C_{rb} was calculated using Eq. 12, where the variables $C_{tot,rb}$, $A_{T,rb}$ and $R_{tot,rb}$ were obtained by numerically solving Eqs. 9–11. $RC_{rb} (= C_{tot,rb} - C_{rb})$ and $R_{rb} = (R_{tot,rb} - RC_{rb})$ were obtained by rearranging Eqs. 7–8. The base model parameters were obtained from the literature [9] and are listed in Table 1. It is assumed that the drug is not endogenously present in all simulations.

Table 1 Base model parameter values used for simulations of the dimensional model

Parameter	Abbreviation	Units	Base value
First-order elimination rate constant from the central compartment	k_{el}	1/h	1.49
First-order tissue distribution rate constant	k_{pt} , k_{tp}	1/h	0.389
Receptor degradation rate constant	k_{deg}	1/h	0.670
Receptor-complex internalization rate constant	k_{int}	1/h	3.16
Equilibrium dissociation rate constant	K_D	nM	1.22
Second-order association rate constant	k_{on}	1/(nM h)	11.3
Initial receptor concentration	R_{ss}	nM	8.19
Volume of the central compartment	V_c	mL/kg	51.2

Values obtained from Mager and Krzyzanski [9]. The value of k_{on} was obtained from Segrave et al. [10]. Molecular weight of the drug is 19710 Da

Simulations were also conducted to calculate the apparent clearance [19] of the drug (CL) for varying doses and the concentration of endogenous receptor concentration (R_{ss}) using the rapid binding model. The apparent clearance is defined in terms of the dose and the area under plasma concentration-time curve of the free drug ($(AUC)_{Cr_b}$) as:

$$CL = \frac{\text{Dose}}{(AUC)_{Cr_b}}, \quad \text{where } (AUC)_{Cr_b} = \int_0^{\infty} C_{rb} dt \quad (31)$$

The dose was varied from 1 to 500 $\mu\text{g}/\text{kg}$ corresponding to a variation of the initial drug concentration in plasma C_i ($= \text{Dose}/V_c$) from 0.991 to 496 nM. R_{ss} was varied from 0.01 to 500 nM. These represent an extreme variation in the two parameters which may not be physiologically relevant; however, the goal of this study was to more fully understand the behavior of the non-linear target mediated system and its effect on pharmacokinetic parameters (CL).

Results

Validity of the rapid binding model

The rapid binding model assumes that the drug–receptor binding is much faster than other processes in the system and requires that the dimensionless parameter ε to be small ($\varepsilon \ll 1$) [9]. A comparison between the dimensionless concentration-time profiles of the rapid binding model and the TMDD model for increasing values of ε is shown in linear and log scales in Figs. 2 and S1. Since ε does not feature in the scaled equations for the rapid binding model (Eqs. 23–30), a single solution from this model is depicted in the figure, whereas different temporal profiles were obtained from the TMDD model for increasing values of ε . Decreasing values of ε , representing smaller binding times, results in lower free drug in the plasma as drug elimination through binding is increased (Figs. 2a and S1A). Thus during the initial time points ($0 < \tau < 1$), the TMDD model predicts a faster decrease in plasma concentrations from an initial value for small values of ε . At $\tau = 0$, the plasma concentration predicted by the rapid binding model is lower than the actual value predicted by the TMDD model. However, the rapid binding solution asymptotically approaches the TMDD solution at later time points. The time (τ_m) required for the rapid binding solution to match the TMDD solution increases with increasing ε . For ε values of 0.01 and 0.1, τ_m is very small (< 0.6) suggesting a close match between the two models.

The temporal profile of the drug–receptor complex obtained from the TMDD model shows an initial rapid increase in concentration followed by a slower decline to baseline at later time points (Figs. 2b and S1B). The rapid binding model closely matches the temporal profile from the TMDD model at later times for small values of ε . However, as expected, it fails to capture the initial rapid increase in the drug–receptor complex and starts at a higher value. Decreasing values of ε in the TMDD

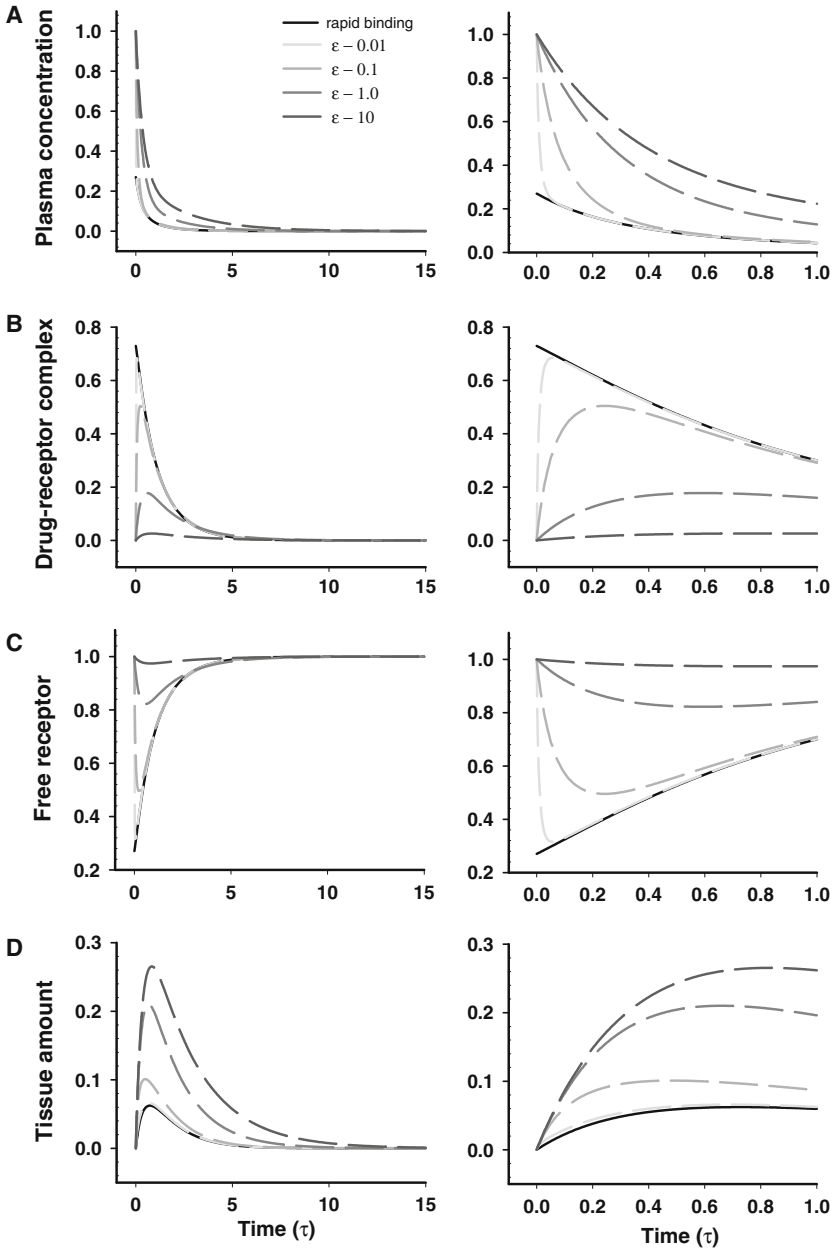


Fig. 2 Comparison between the rapid binding (*solid curve*) and full TMDD models (*dashed curve*) for increasing values of the parameter ε (0.01, 0.1, 1.0 and 10). Simulated dimensionless concentration–time profiles of **a** free drug in plasma [c , c_{rb}], **b** the drug-receptor complex [rc , rc_{rb}], **c** free receptor pool [r , r_{rb}] and **d** drug in tissue [a_T , $a_{T,rb}$]. The right panels in each panel represent profiles during the initial time. All other parameter values were fixed to 1 except for $\lambda = 0.1$

model, again representing smaller binding times, results in an increase in formation of the drug–receptor complex.

In the case of the free receptor, effects opposite to those described for the drug–receptor complex were observed. The temporal profile of the free receptor obtained from the TMDD model shows an initial rapid decrease in its concentration followed by a slower increase to baseline at later time points (Figs. 2c and S1C). The rapid binding model closely matches this temporal profile at later times for small values of ε . However, as expected, it fails to capture the initial rapid decline in the free receptor and starts at a lower value. The temporal profile of the tissue compartment shows that decreasing values of ε in the TMDD model also results in decreased drug accumulation in the tissue compartment (Figs. 2d and S1D). Overall, there was good agreement between the two models for small values ε (0.01 and 0.1), with slight deviations at early time points, for each state variable.

Effect of parameter variation on the rapid binding model

Simulations using scaled equations were performed to assess the effect of other model parameters on the agreement between the rapid binding and TMDD models (Figs. 3, 4, S2 and S3). Each parameter β , γ , δ , κ , λ , and μ was varied from 0.01 to 10, one at a time, while the values of ε and λ were fixed to 0.1 and other parameters to 1. Overall, there was good agreement between the temporal profiles of free drug in plasma over the entire range of parameter values with slight deviations at early time points, as seen in Figs. 3 and 4 that show the simulated curves in the linear scale. Differences between the rapid binding and TMDD models for large times in the logarithmic scale become smaller if the parameter values decreased from 0.1 to 0.01, except for γ and λ . The profiles from the rapid binding model reasonably approach the solution from the TMDD model within $\tau < 1$ as observed in the linear scale. Similar results were obtained for the drug–receptor complex, free receptor, and drug in the tissue compartment (data not shown).

Effect of dose on the rapid binding approximation

For nonlinear systems, dose is an important variable that can significantly alter drug exposure and consequently the response. The temporal profiles for free plasma LIF concentrations for increasing doses (12.5–500 $\mu\text{g}/\text{kg}$), using parameter values in Table 1, are shown in Figs. 5a and S4A. The profiles exhibit poly-exponential behavior with an initial distribution phase followed by an intermediate non-linear receptor saturation phase and a prolonged terminal elimination phase. Slight deviations are observed between the two models only during the initial time points ($0 < t < 0.05$ h). The rapid binding model under predicts the drug concentrations initially, and this effect is more pronounced for low doses. For this case, the free drug plasma profiles are well predicted by the rapid binding model even at low drug concentrations during the terminal phase (Fig. S4A).

The simulated temporal profiles of the drug–receptor complex from the TMDD model shows an initial rapid increase from baseline due to the fast binding of the drug to the receptor and a subsequent decline, which is indicative of much slower

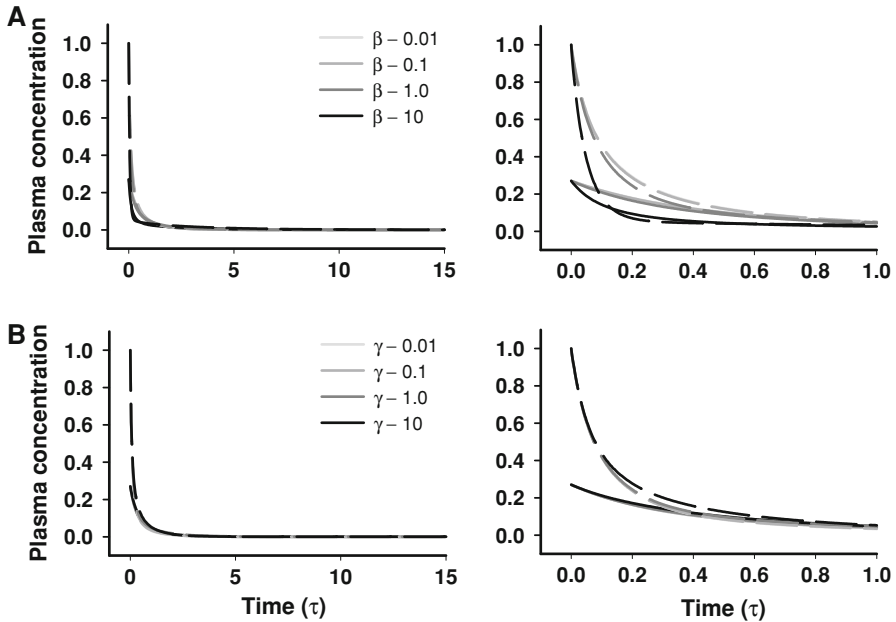


Fig. 3 Comparison between the rapid binding (*solid curve*) and the full TMDD models (*dashed curve*) for increasing values of linear distribution parameters. Simulated dimensionless concentration-time profiles of free drug in the plasma [c , c_{fb}] for increasing values (0.01, 0.1, 1.0 and 10) of **a** β and **b** γ . The right panels in each represent profiles during the initial time. The value of ε and λ were fixed to 0.1 and all other parameters to 1

internalization, degradation and the dissociation of drug–receptor complex at later times (Figs. 5b and S4B). The profiles from the rapid binding model capture all these essential features except the initial rise in concentrations from $t = 0$ to about 0.05 h. The profiles in the rapid binding case, although start at high values, asymptotically approach the TMDD profiles after initial time points.

The simulated temporal profiles of the free receptor from the TMDD model show a sharp initial decline due to drug–receptor binding and a subsequent steady increase in the receptor concentration toward baseline value owing to slower receptor synthesis (Figs. 5c and S4C). As observed for the drug–receptor complex, the profiles from the rapid binding-model capture all the essential features except the initial decline in concentrations from $t = 0$ to about 0.05 h. The profiles from the rapid binding model start at low values, and agreement with the profiles from the TMDD model was observed only after the initial time points. Close agreement between temporal profiles of the drug concentration in tissues is observed for all dose levels (Figs. 5d and S4D).

These simulations show that the rapid binding model closely approximates the exact solution of TMDD for a range of physiologically relevant doses. This is of particular significance because dose can represent a critical design consideration in pharmacokinetic studies.

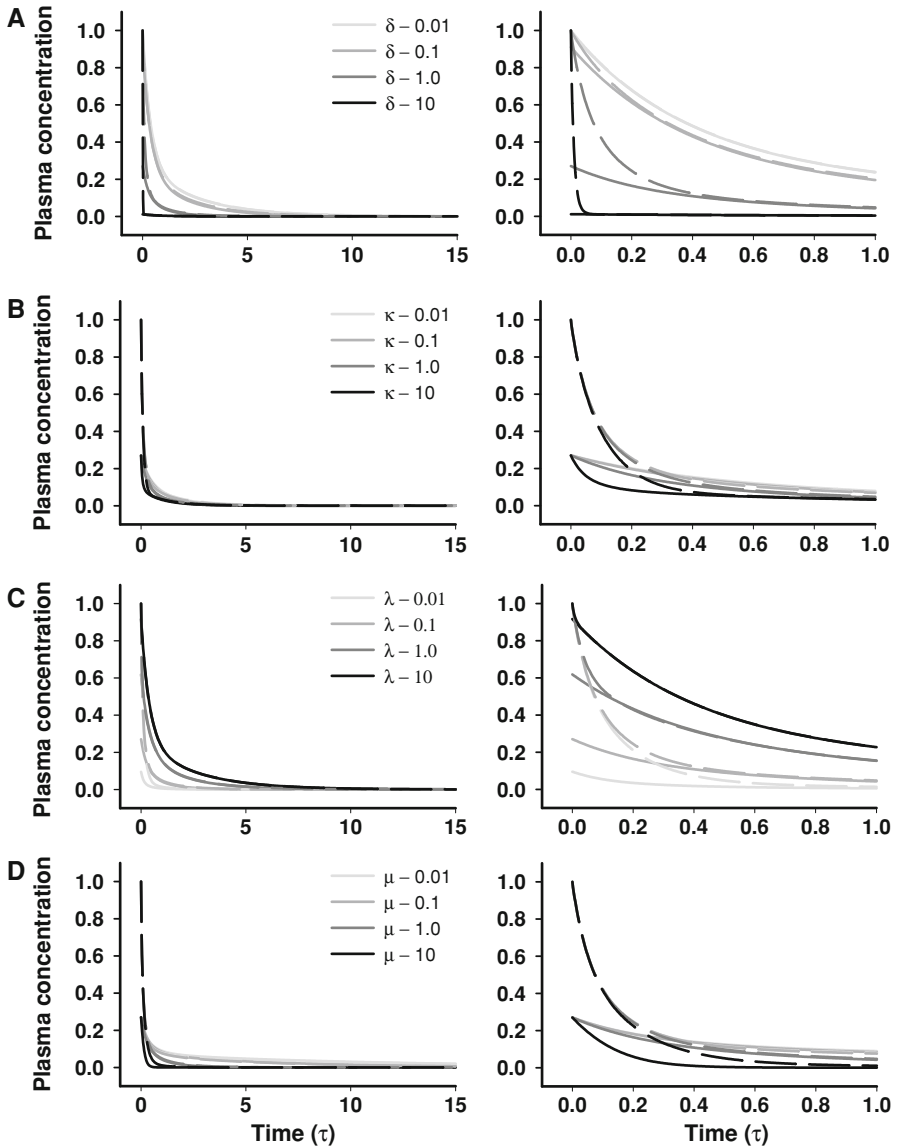


Fig. 4 Comparison between the rapid binding (*solid curve*) and full TMDD models (*dashed curve*) for increasing values of nonlinear binding parameters. Simulated dimensionless concentration-time profiles of free drug in the plasma [c , c_{fb}] for increasing values (0.01, 0.1, 1.0 and 10) of **a** δ , **b** κ , **c** λ and **d** μ . The right panels in each represent profiles during the initial time. The value of ϵ and λ were set to 0.1, and all other parameters in each case were fixed to 1

Effect of dose and receptor density on clearance

The apparent clearance (CL) of drugs exhibiting target-mediated disposition decreases with increasing dose levels [1, 2] when binding of the drug invokes a

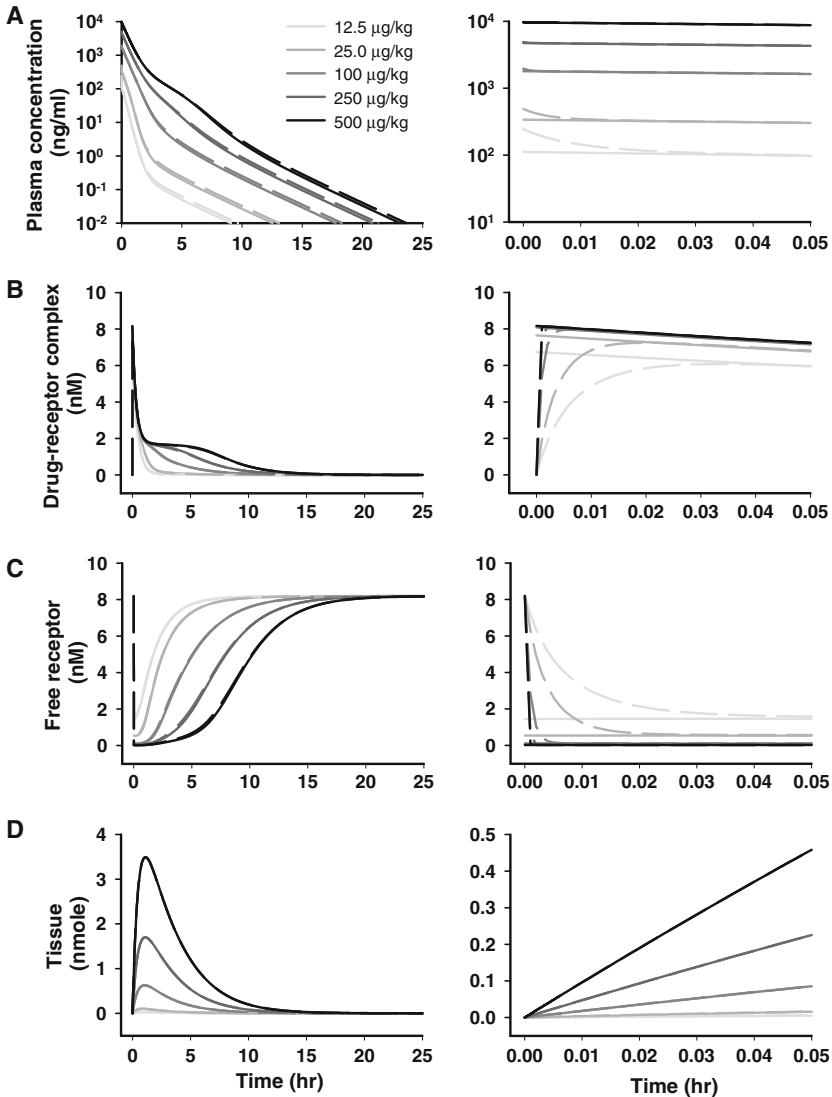


Fig. 5 Comparison between the rapid binding (*solid curve*) and full TMDD models (*dashed curve*) for increasing doses (12.5, 25, 100, 250, and 500 $\mu\text{g}/\text{kg}$). Simulated concentration-time profiles of **a** free drug in plasma [C , C_{rb}], **b** drug-receptor complex [RC , RC_{rb}], **c** free receptor pool [R , R_{rb}], and **d** drug in tissue [A_{T} , $A_{\text{T,rb}}$]. The right panels in each represent profiles during the initial time. Model parameters correspond to those previously determined for leukemia inhibitory factor [9] shown in Table 1

major elimination pathway. The rapid binding model can be used to show that both the linear clearance from the central compartment, given by $k_{\text{el}}V_c$, and the non-linear clearance due to the internalization of the drug–receptor complex (k_{int}) contribute to the apparent clearance of target mediated drugs:

$$CL = k_{el}V_c + k_{int}V_c \frac{(AUC)_{RCrb}}{(AUC)_{Crb}} \quad (32)$$

where $(AUC)_{Crb}$ and $(AUC)_{RCrb}$ represent the area under concentration versus time profiles of the free drug and drug–receptor complex. The derivation of Eq. 32 is provided in Appendix 1. This relationship suggests that for the limiting case of large doses, $(AUC)_{RCrb}$ would be negligible compared to $(AUC)_{Crb}$ and thus apparent CL would approach the linear clearance component. Simulations of signature temporal profiles of C_{rb} and RC_{rb} (Fig. 5) show that the ratio $(AUC)_{RCrb}/(AUC)_{Crb}$ varies from 1.55 for the low dose (12.5 $\mu\text{g}/\text{kg}$) to 0.0565 for the high dose (500 $\mu\text{g}/\text{kg}$) confirming a decrease in clearance with increasing dose levels as expected. Equation 32 supports the concept that degradation/internalization of the drug–receptor complex is required to observe a decrease in apparent clearance with increasing dose [2]. In absence of internalization of the drug–receptor complex (i.e., $k_{int} = 0$), apparent CL is the same as linear clearance.

Since binding of the drug is capacity limited by the endogenous level of the receptor pool (R_{ss}), possibly influencing $(AUC)_{RCrb}$, R_{ss} would be expected to influence the pharmacokinetic properties of the drug. Simulations were performed to calculate the apparent clearance by varying the two critical parameters, Dose and R_{ss} simultaneously and plotting a 3-dimensional map of CL versus R_{ss} versus Dose/V_c , where Dose/V_c ($= C_i$) is the initial free drug concentration in the central compartment (Fig. 6). Dose/V_c was plotted on the y-axis as it reflects both the administered dose and maximal plasma concentration (initial concentration for this case) and has units of concentration (nM), which is consistent with R_{ss} . Dose and the initial free drug concentration C_i have been used interchangeably in the text below.

Simulations show that the clearance varied from 1.25 to 1051 mL/min/kg by simultaneously varying R_{ss} (from 0.01 to 500 nM) and dose (from 500 to 1 $\mu\text{g}/\text{kg}$). Corresponding variation in Dose/V_c is from 496 to 0.991 nM. These extreme variations, although not physiological, were critical for understanding the properties of this non-linear system. In Fig. 6, clearance is encoded in terms of gray color, increasing from black \rightarrow gray. Drug clearance was shown to be high for the highest R_{ss} ($\approx 500\text{nM}$) and the lowest dose (≈ 1 nM) in a 3-D plot (Fig. 6a) and its projection (Fig. 6b). For a given receptor density R_{ss} , increasing dose causes the clearance to decline owing to receptor saturation. Similarly, at a particular dose level (represented by constant Dose/V_c), decreasing R_{ss} exhibits the same qualitative effect of decreasing clearance given the likelihood of saturating lower levels of receptors.

The accuracy of the rapid binding is dependent on the assumption of comparable or lower level of receptor concentration than drug concentration, given by the relationships $\delta = O(1)$ or $R_{ss} = k_{syn}/k_{deg} = O(\text{Dose}/V_c)$ [9]. This assumption states that the ratio $(R_{ss}/(\text{Dose}/V_c))$ is bound by a constant without specifying the value of the constant. However, this is only partly maintained for these calculations. In order to determine the region of applicability of the rapid binding model, it is assumed that the value of the constant is 1. Although the actual value can be greater than 1, it is conservatively assumed to be 1 for these calculations. In Fig. 6c only the region where $R_{ss}/(\text{Dose}/V_c) \leq 1$ has been represented. The black color of the map

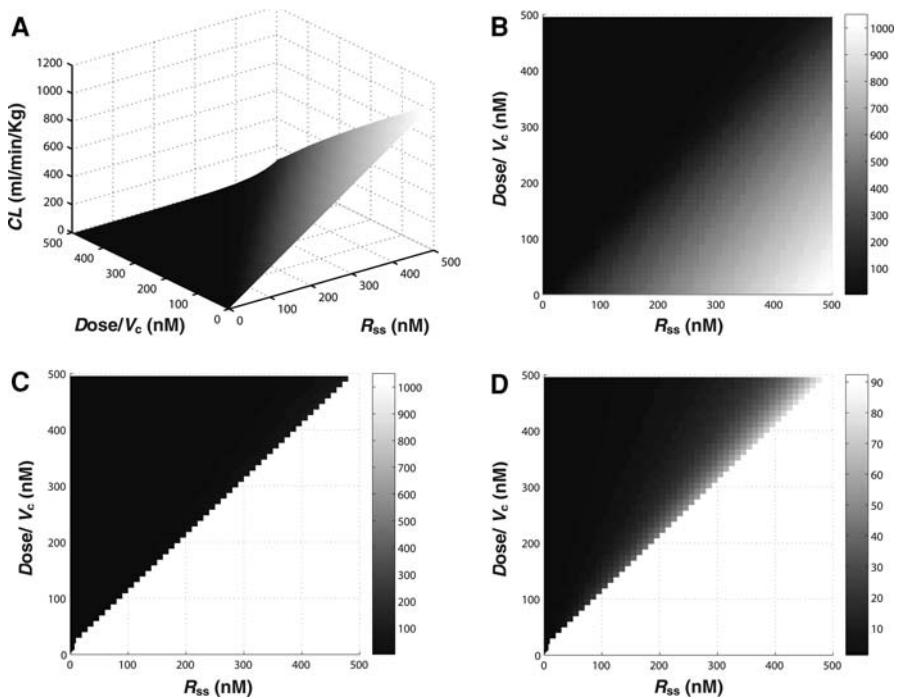


Fig. 6 Effect of the endogenous receptor concentration and dose on clearance. **a** 3-D map of clearance [CL] with dose [$Dose/V_c$] and the endogenous receptor concentration [R_{ss}]. **b** 2-D projection of the map on the $x - y$ ($[R_{ss}] - [Dose/V_c]$) plane. **c** 2-D projection with boundary defining the region of validity of the rapid binding model. **d** 2-D projection map for varying clearance in the region confirming the assumptions of the rapid binding model

gives an impression that the clearance remained constant in this region. However, it is important to note that the clearance varied significantly from 1.25 to 92.4 mL/min/kg in this region and for better visualization, it is plotted on a reduced scale in Fig. 6d. The overall pattern of CL is conserved and declines with increasing dose or decreasing R_{ss} .

In Appendix 2 we show that as the small parameter δ ($= R_{ss}/(Dose/V_c)$) approaches zero, which represents very low receptor levels compared to dose, the rapid binding model reduces to a two compartmental linear model comprising of a central and a tissue compartment [19]. The clearance in such cases (i.e., large dose relative to free receptors) thus approaches the standard linear clearance from the central compartment given by $k_{el}V_c$. Clearly δ can approach zero either due to a very large dose that saturates the receptors or the presence of very low levels of receptors.

The expected profile of decreasing clearance with increasing dose levels is shown by simulation in Fig. 7. The limit of clearance for high doses as defined by $k_{el}V_c$ closely approximates the simulated curve. The vertical line in Fig. 7, at a dose that is equivalent to the endogenous receptor concentration (R_{ss}), defines the domain of

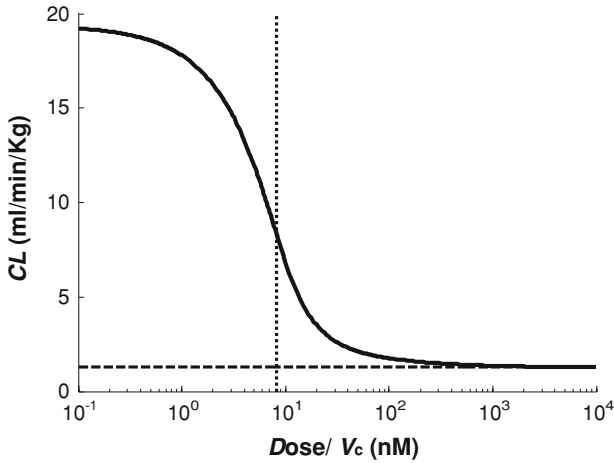


Fig. 7 Effect of increasing dose ($Dose/V_c$) on clearance (CL). The thick solid line was obtained numerically by solving the rapid binding model. The dashed horizontal line represents the linear clearance ($k_{el}V_c$) for the limiting case of high dose relative to receptor concentration. The dotted vertical line at a dose that is equivalent to the endogenous receptor concentration (R_{ss}) defines the domain of validity of the rapid binding model. This region lies to the right of the vertical line

validity of the rapid binding model. The valid domain consistent with the underlying assumption, $R_{ss} = k_{syn}/k_{deg} = O(Dose/V_c)$, lies to the right of the vertical line.

Discussion

This study provides a numerical validation of the rapid binding approximation of a TMDD model. The assumption of rapid-binding $\epsilon \rightarrow 0$, implies that ϵ must be small for the rapid binding approximation to be appropriate. This was confirmed numerically by simulations where close agreement between the rapid binding model and TMDD model was observed for smaller values of ϵ (0.01 and 0.1) when all other model parameter values were fixed to 1 and λ to 0.1 (Figs. 2 and S1). Also, the time required for the rapid binding solution to match the TMDD solution decreases significantly with decreasing ϵ .

The values of the parameters ϵ and δ were calculated using Eq. 21 for six different drugs that exhibit target mediated drug disposition (Table 2). ϵ values were less than 0.1 for all drugs for intermediate and high dose levels. At low dose levels, LIF, TRX1 (an anti-CD4 monoclonal antibody), and interferon- β have $\epsilon < 0.1$, whereas values of ϵ range between 0.246 and 0.552 for erythropoietin, imirestat and bosentan. The calculated values of δ for these drugs range between 4.32×10^{-3} and 12.5.

The choice of using $1/k_{el}$ as the scaling parameter for time is reasonable; however, for some TMDD pharmacokinetic models (e.g., thrombopoietin), k_{el} is 0 suggesting negligible linear elimination (e.g. renal) of the drug from the plasma

Table 2 Calculated values of ε and δ for selected TMDD drugs at varying dose levels

Drug/ parameter	ε low dose	ε intermediate dose	ε high dose	δ low dose	δ intermediate dose	δ high dose
LIF	1.14×10^{-2}	1.43×10^{-3}	2.86×10^{-4}	4.45×10^{-1}	5.56×10^{-2}	1.11×10^{-2}
TRX1	6.48×10^{-4}	1.30×10^{-4}	6.48×10^{-5}	3.43×10^{-1}	6.87×10^{-2}	3.43×10^{-2}
EPO	5.52×10^{-1}	1.23×10^{-2}	1.36×10^{-3}	1.75×10^0	3.89×10^{-2}	4.32×10^{-3}
IFN- β	7.06×10^{-2}	2.35×10^{-2}	7.06×10^{-3}	1.83×10^0	6.10×10^{-1}	1.83×10^{-1}
Imirestat	2.46×10^{-1}	2.46×10^{-2}	9.82×10^{-3}	1.25×10^1	1.25×10^0	4.99×10^{-1}
Bosentan	4.63×10^{-1}	1.85×10^{-2}	6.18×10^{-3}	2.33×10^0	9.3×10^{-2}	3.1×10^{-2}

Values of ε and δ were calculated according to Eq. 21 using previously determined parameter values for LIF, leukemia inhibitory factor, in sheep [10], TRX1, an anti-CD4 monoclonal antibody, in humans [8], EPO, erythropoietin, in rats [21], interferon (IFN)- β in cynomolgus monkeys [22], and imirestat and bosentan in healthy volunteers [2]

[20]. In such cases, k_{int} can be used as an alternative time scale as one of the elimination pathways must be present to have an output from the system.

The robustness of the rapid binding model was also challenged by varying the values of each of the model parameters (β , γ , δ , κ , λ , and μ) from 10 to 0.01 while fixing the value of ε and λ to 0.1. Close agreement was observed for the rapid binding and TMDD models for these simulations (Figs. 3 and 4) with some discrepancies observed only in the logarithmic scale that diminish with decreasing parameter values (Figs. S2 and S3). Similar results were obtained for escalating doses with closer agreement between the two models for higher doses (Figs. 5 and S4).

Decreasing clearance with increasing dose and decreasing R_{ss} (Fig. 6) indicates that for drugs exhibiting TMDD, the relative ratio of the endogenous receptor concentration and dose is an important determinant of the pharmacokinetic properties (CL), rather than the individual parameters, and should be carefully accounted for in experimental designs. The derived limit of clearance for large doses relative to R_{ss} , closely matched the numerical value (Fig. 7). At large doses, the rapid binding model reduces to a two-compartmental linear model comprising of a central and tissue compartment and the clearance in such cases approaches the standard linear clearance. Overall, this study provides better understanding of the validity of the rapid binding model and its mathematical properties pertinent to effective implementation of the model for drugs exhibiting target mediated drug disposition.

Acknowledgements This study was supported by Grant GM57980 (for D.E.M. and W.K.) and funds for a postdoctoral fellowship from Amgen, Inc. (to A.M.).

Appendix 1

Derivation of apparent clearance for the rapid binding model

In order to obtain an analytical solution for clearance of the rapid binding model, Eqs. 9 and 10 are integrated:

$$\int_0^\infty \frac{dC_{\text{tot,rb}}}{dt} dt = \int_0^\infty \left(-k_{\text{int}}C_{\text{tot,rb}} - (k_{\text{el}} + k_{\text{pt}} - k_{\text{int}})C_{\text{rb}} + k_{\text{tp}} \frac{A_{\text{T,rb}}}{V_c} \right) dt \tag{33}$$

$$\int_0^\infty \frac{dA_{\text{T,rb}}}{dt} dt = \int_0^\infty (k_{\text{pt}}C_{\text{rb}}V_c - k_{\text{tp}}A_{\text{T,rb}}) dt \tag{34}$$

Multiplying Eq. 33 by V_c and adding to Eq. 34 yields the following relation:

$$\text{Dose} = k_{\text{el}}V_c \int_0^\infty C_{\text{rb}} dt + k_{\text{int}}V_c \int_0^\infty (C_{\text{tot,rb}} - C_{\text{rb}}) dt \tag{35}$$

Here, $\int_0^\infty C_{\text{rb}} dt$ represents the area under the plasma concentration-time curve of the free drug ($(AUC)_{\text{Crb}}$). Substituting Eq. 7, in $\int_0^\infty (C_{\text{tot,rb}} - C_{\text{rb}}) dt$ yields the term, $\int_0^\infty (RC_{\text{rb}}) dt$, which represents the area under the concentration-time curve of the drug–receptor complex ($(AUC)_{\text{RCrb}}$). Dividing Eq. 35 by the $(AUC)_{\text{Crb}}$ gives the apparent clearance of the target mediated drug as:

$$CL = k_{\text{el}}V_c + k_{\text{int}}V_c \frac{(AUC)_{\text{RCrb}}}{(AUC)_{\text{Crb}}} \tag{36}$$

Appendix 2

Large dose approximation of the rapid binding model

It is important to understand the limiting behavior of the rapid binding model for very large dose level compared to the endogenous receptor concentration. For the limiting case of very large dose relative to $R_{\text{ss}} (= k_{\text{syn}}/k_{\text{deg}})$, the dimensionless parameter, δ given by Eq. 21 is a small parameter. Mathematically, this is represented as:

$$\delta = \frac{k_{\text{syn}}}{k_{\text{deg}}(\text{Dose}/V_c)} \ll 1 \tag{37}$$

Eqs. 23 and 29 imply that

$$r_{\text{Crb}} = \frac{r_{\text{tot,rb}}c_{\text{rb}}}{\lambda + c_{\text{rb}}} \tag{38}$$

Consequently, Eq. 26 can be transformed to a δ free form

$$\frac{dr_{\text{tot,rb}}}{d\tau} = \kappa - \frac{(\mu - \kappa)r_{\text{tot,rb}}c_{\text{rb}}}{\lambda + c_{\text{rb}}} - \kappa r_{\text{tot,rb}} \tag{39}$$

Since the solution of the system of differential Eqs. 23–26 continuously depend on δ , one can obtain the large dose approximation by letting $\delta \rightarrow 0$. Thus, Eqs. 27 and 28 show that the free drug concentration is equal to the total drug concentration

$$c_{\text{tot,rb}} = c_{\text{rb}} \quad (40)$$

Substituting Eq. 40 in Eqs. 24 and 25 results in the following set of differential equations that represent the governing equations of a two compartmental linear model with linear elimination only from the central compartment:

$$\frac{dc_{\text{rb}}}{d\tau} = -(1 + \beta)c_{\text{rb}} + \gamma a_{\text{T,rb}} \quad (41)$$

$$\frac{da_{\text{T,rb}}}{d\tau} = \beta c_{\text{rb}} - \gamma a_{\text{T,rb}} \quad (42)$$

The clearance (CL), and steady-state volume of distribution (V_{ss}) of a two compartmental linear system has been well established [19] and in dimensional form, they are as follows:

$$CL = V_c k_{\text{el}} \quad (43)$$

$$V_{\text{ss}} = V_c \left(1 + \frac{k_{\text{pt}}}{k_{\text{tp}}} \right) \quad (44)$$

References

1. Levy G (1994) Pharmacologic target-mediated drug disposition. *Clin Pharmacol Ther* 56:248–252
2. Mager DE, Jusko WJ (2001) General pharmacokinetic model for drugs exhibiting target-mediated drug disposition. *J Pharmacokinet Pharmacodyn* 28:507–532. doi:[10.1023/A:1014414520282](https://doi.org/10.1023/A:1014414520282)
3. Sugiyama Y, Hanano M (1989) Receptor-mediated transport of peptide hormones and its importance in the overall hormone disposition in the body. *Pharm Res* 6:192–202. doi:[10.1023/A:1015905331391](https://doi.org/10.1023/A:1015905331391)
4. Lobo ED, Hansen RJ, Balthasar JP (2004) Antibody pharmacokinetics and pharmacodynamics. *J Pharm Sci* 93:2645–2668. doi:[10.1002/jps.20178](https://doi.org/10.1002/jps.20178)
5. Tang L, Persky AM, Hochhaus G, Meibohm B (2004) Pharmacokinetic aspects of biotechnology products. *J Pharm Sci* 93:2184–2204. doi:[10.1002/jps.20125](https://doi.org/10.1002/jps.20125)
6. Mager DE (2006) Target-mediated drug disposition and dynamics. *Biochem Pharmacol* 72:1–10. doi:[10.1016/j.bcp.2005.12.041](https://doi.org/10.1016/j.bcp.2005.12.041)
7. Jonsson EN, Macintyre F, James I, Krams M, Marshall S (2005) Bridging the pharmacokinetics and pharmacodynamics of UK-279, 276 across healthy volunteers and stroke patients using a mechanistically based model for target-mediated disposition. *Pharm Res* 22:1236–1246. doi:[10.1007/s11095-005-5264-x](https://doi.org/10.1007/s11095-005-5264-x)
8. Ng CM, Stefanich E, Anand BS, Fielder PJ, Vaickus L (2006) Pharmacokinetics/pharmacodynamics of nondepleting anti-CD4 monoclonal antibody (TRX1) in healthy human volunteers. *Pharm Res* 23:95–103. doi:[10.1007/s11095-005-8814-3](https://doi.org/10.1007/s11095-005-8814-3)
9. Mager DE, Krzyzanski W (2005) Quasi-equilibrium pharmacokinetic model for drugs exhibiting target-mediated drug disposition. *Pharm Res* 22:1589–1596. doi:[10.1007/s11095-005-6650-0](https://doi.org/10.1007/s11095-005-6650-0)
10. Segrave AM, Mager DE, Charman SA, Edwards GA, Porter CJ (2004) Pharmacokinetics of recombinant human leukemia inhibitory factor in sheep. *J Pharmacol Exp Ther* 309:1085–1092. doi:[10.1124/jpet.103.063289](https://doi.org/10.1124/jpet.103.063289)
11. Bauer RJ, Dedrick RL, White ML, Murray MJ, Garovoy MR (1999) Population pharmacokinetics and pharmacodynamics of the anti-CD11a antibody hu1124 in human subjects with psoriasis. *J Pharmacokinet Biopharm* 27:397–420. doi:[10.1023/A:1020917122093](https://doi.org/10.1023/A:1020917122093)
12. Lees KR, Kelman AW, Reid JL, Whiting B (1989) Pharmacokinetics of an ACE inhibitor, S-9780, in man: evidence of tissue binding. *J Pharmacokinet Biopharm* 17:529–550. doi:[10.1007/BF01071348](https://doi.org/10.1007/BF01071348)

13. Levy G, Mager DE, Cheung WK, Jusko WJ (2003) Comparative pharmacokinetics of coumarin anticoagulants L: Physiologic modeling of S-warfarin in rats and pharmacologic target-mediated warfarin disposition in man. *J Pharm Sci* 92:985–994. doi:[10.1002/jps.10345](https://doi.org/10.1002/jps.10345)
14. Gibiansky L, Gibiansky E, Kakkar T, Ma P (2008) Approximations of the target-mediated drug disposition model and identifiability of model parameters. *J Pharmacokinet Pharmacodyn* 35:573–591. doi:[10.1007/s10928-008-9102-8](https://doi.org/10.1007/s10928-008-9102-8)
15. Yan X, Mager DE, Krzyzanski W (2008) Selection between Michaelis-Menten and target-mediated drug disposition pharmacokinetic models. *AAPS J* 10(S2)
16. Tzafiriri AR (2003) Michaelis-Menten kinetics at high enzyme concentrations. *Bull Math Biol* 65:1111–1129. doi:[10.1016/S0092-8240\(03\)00059-4](https://doi.org/10.1016/S0092-8240(03)00059-4)
17. Tzafiriri AR, Edelman ER (2004) The total quasi-steady-state approximation is valid for reversible enzyme kinetics. *J Theor Biol* 226:303–313. doi:[10.1016/j.jtbi.2003.09.006](https://doi.org/10.1016/j.jtbi.2003.09.006)
18. Tzafiriri AR, Edelman ER (2005) On the validity of the quasi-steady state approximation of bimolecular reactions in solution. *J Theor Biol* 233:343–350. doi:[10.1016/j.jtbi.2004.10.013](https://doi.org/10.1016/j.jtbi.2004.10.013)
19. Gibaldi M, Perrier D (1982) *Pharmacokinetics*. Marcel Drekker, Inc, New York
20. Jin F, Krzyzanski W (2004) Pharmacokinetic model of target-mediated disposition of thrombopoietin. *AAPS PharmSci* 6:E9. doi:[10.1208/ps060109](https://doi.org/10.1208/ps060109)
21. Woo S, Krzyzanski W, Jusko WJ (2007) Target-mediated pharmacokinetic and pharmacodynamic model of recombinant human erythropoietin (rHuEPO). *J Pharmacokinet Pharmacodyn* 34:849–868. doi:[10.1007/s10928-007-9074-0](https://doi.org/10.1007/s10928-007-9074-0)
22. Mager DE, Neuteboom B, Efthymiopoulos C, Munafo A, Jusko WJ (2003) Receptor-mediated pharmacokinetics and pharmacodynamics of interferon-beta1a in monkeys. *J Pharmacol Exp Ther* 306:262–270. doi:[10.1124/jpet.103.049502](https://doi.org/10.1124/jpet.103.049502)